Olin-NASA Research Group

# XACT Alignment System

Final Report and Test Apparatus Documentation

Raphael Cherney, Daniel Elg, Clayton Gimenez, Steven Higgins
10/18/2009

# Table of Contents


Summary ..... 3
- XACT Rocket ..... 3
- System Requirements ..... 4

System Design ..... 4
- Proposed Setup ..... 4
- Revised Setup ..... 5
- Geometry ..... 6
- Position Sensitive Photodiodes ..... 7
  - Principles of Operation ..... 7
  - Calibration ..... 7

Testing Apparatus ..... 10
- Circuitry ..... 13
- Interface Board ..... 14
- Code ..... 14

Results ..... 15
- Laser Dispersion ..... 17

Spaceflight Considerations ..... 18

System Improvements ..... 18

Appendix – Additional Diagrams, Figures, and Information ..... 19
- XACT Interface Board Circuit Schematic ..... 19
- XACT Interface Board PCB Layout ..... 20
- Test Apparatus Example Setup ..... 21

Acknowledgements ..... 21

Concluding Note ..... 22

# Summary

The X-Ray Advanced Concepts Testbed sounding rocket project is a Goddard Space Flight Center program intended to provide low cost x-ray telescopy using sounding rockets as platforms for imaging, as well as developing and testing new equipment for x-ray astronomy. Sounding rockets are comparatively low-cost sub-orbital rockets that reach their target height in under a minute, then hold altitude for about five minutes before returning to earth. Due to their low cost and repeatability on short time intervals, they are well suited to repeated experiments, data collection, and equipment testing. However, they pose problems for x-ray imaging. X-ray telescopes use shallow angle mirrors that must be kept in alignment down to fractions of millimeters and degrees or else image quality is lost. Unfortunately, sounding rocket payloads can fall out of alignment under the stresses and vibrations of launch. Thus, the goal of the XACT Optical Alignment System Project is to design and develop a proof of concept of a system that can detect such minor displacements between the ends of the rocket and save the data for later image correction.

# XACT Rocket

Figure 1: CAD Model of XACT Sounding Rocket

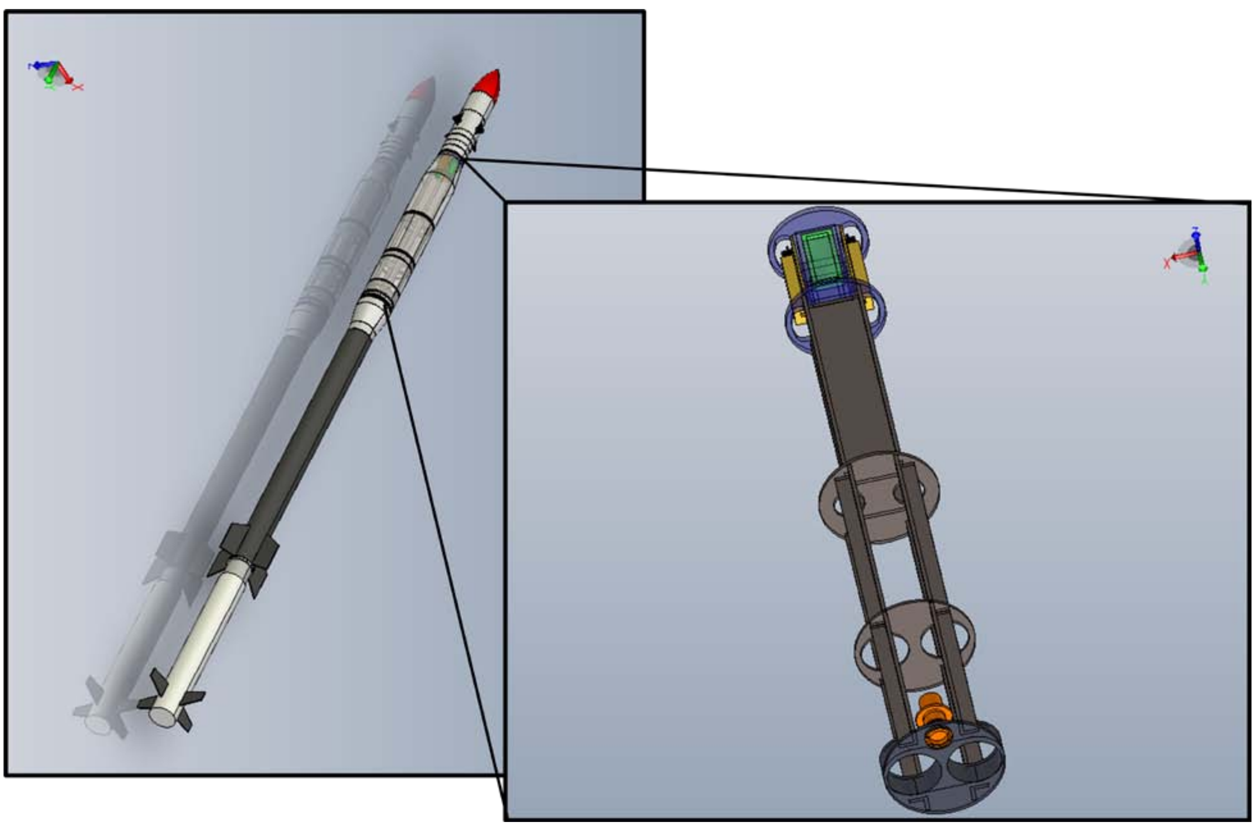

Table I: XACT Rocket Specifications

| | |
|---|---|
| **Payload Length** | 3.36 m |
| **Payload Diameter** | 0.56 m |
| **Payload Mass** | 80.2 kg |

The XACT sounding rocket is a standard Black Brant IX rocket, as seen in Figure 1. The payload consists of three main elements: x-ray collectors, x-ray detectors, and a star tracker. The star tracker is aligned with the collectors in order to determine the target of the telescope from the position of various stars. The collectors consist of the necessary shallow angle mirrors to deflect the x-rays in and down to the detectors at the opposite end of the payload. As currently envisioned, the payload is approximately 3 meters long and 0.5 meters in diameter. An expanded view of the payload can also be seen in Figure 1. All the parts are mounted in a frame to keep the collectors in line with the detectors in order to produce clear images. However, during launch the two ends of the payload (the collectors and the detectors) may come out of alignment in various ways. As such, some method of determining the misalignment is necessary if clear images of the desired target are to be obtained. In the case of the XACT project, it was determined that an optical bench-based alignment system was the preferred solution. This system would use sensors to detect very small displacements of a laser dot as the rocket launches in order to determine the misalignment.

## System Requirements

Specifically, in order to ensure accurate results and calibration with the star tracker, the x-ray concentrators and detectors must not shift laterally more than 1 mm nor tilt more than 2 arcminutes relative to each other. To ensure that these specifications are met, displacements should be measurable to 0.1 mm and tilts to 0.2 arcminutes.

As such, the NASA-Olin XACT Optical Alignment System Project had four major goals:

- The alignment system must fit the geometry of the sounding rocket (i.e. 3 meters between benches and 0.5 meter payload diameter).
- X/Y displacement must be read to an accuracy of 0.1 mm.
- X/Y tip and tilt must be read to an accuracy of 0.2 arcminutes.
- Displacements and tip/tilts should optimally be read at 1 kHz and stored for later use.

With these goals in mind, the team developed the following final Statement of Work:

> Design and test a working prototype optical bench system with approximately three meters separation capable of detecting x and y offsets and tip and tilt angles over time at a rate of 1 kHz. The x and y offset readings will be accurate to 0.1 mm and angle readings to 0.2 arcminutes. The system will analyze the raw data from the system and record the offset and angular displacement.

# System Design

## Proposed Setup

During the 2008 Olin-NASA Solar Sensor Project, position sensitive photodiodes (PSDs) were found to be an ideal sensor for detecting light sources and reading minor changes. Additionally, they were provided initially by our mentor at Goddard Space Flight Center. Thus, moving forward, the major challenges of the physical system were determining a geometry that would allow the four required displacements to be solved for and then solving that geometry. The initially recommended geometry placed both PSDs and the laser on one end of the system, with several mirrors on the opposite side, as seen below.

**Figure 2: Initial Proposed System Geometry**

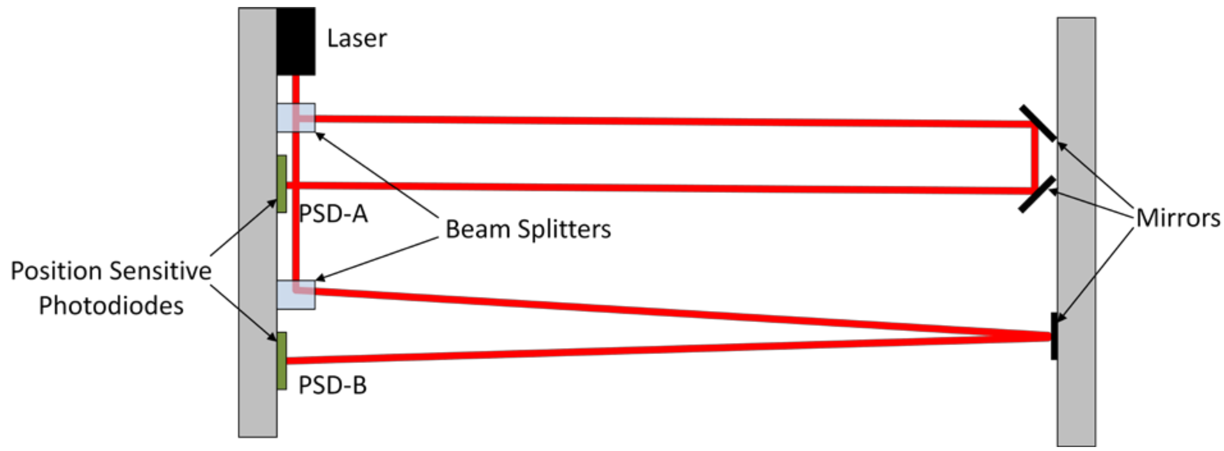


However, it soon became apparent that this geometry did not create a system of equations that could be resolved. Instead, every displacement affected all others significantly enough to make it impossible to exclusively resolve the system. Furthermore, the necessity of a conical mirror opposite PSD-A complicated the geometry significantly. As a consequence, the physical set-up was redesigned.

## Revised Setup

Instead of both PSDs mounted on the same end, they were split and placed on either side of the system, as seen below. This change allowed the laser to shine directly on one of the PSDs for an immediate reading of X/Y displacement. This reading is slightly effected by tip and tilt of the benches, but it was determined that this error in displacement was too small to be resolved by the PSDs. (For a more in-depth explanation see the Geometry Report).

**Figure 3: Modified System Geometry**

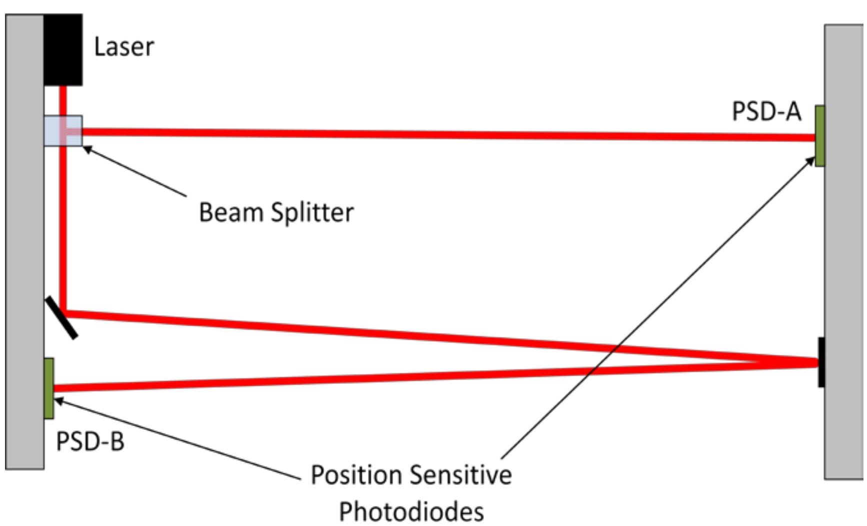

Thus, a simple change allowed the system to become uniquely solvable, since the readings of PSD-B would be interpreted solely to find X/Y tip and tilt, with the X/Y displacement values already known directly from PSD-A. The next major step was to determine the exact relations between the PSD readings.

## Geometry

To find the expressions necessary to define X/Y tip and tilt in terms of X/Y displacement and constants of the system, we returned to basic geometry and applied it to a complicated problem. Working through it bit by bit, we slowly built a complete answer using the Law of Sines and basic angle properties, such as vertical angles, complementary/supplementary angles, the properties of triangles, and the reflection characteristics of plane mirrors. For the details of the derivation, see the XACT Geometry Report. In the end, however, the following expressions were obtained for $dx$ and $dy$, the X/Y tip and tilt sensor readings from PSD B:

$$dx = \frac{\left(\frac{l}{\cos\alpha} + \frac{(r-\Delta x)\sin\theta}{\sin(90-2\theta-\alpha)} + \frac{\Delta y\tan\phi}{\cos\alpha}\right)\sin(2(\theta+\ \alpha))}{\sin\,(90-2\theta-\alpha)} - \ d$$

$$dy = \left(l + \Delta y\tan\phi + \frac{(r-\Delta x)\sin\theta\cos\alpha}{\sin\ (90-\theta-\alpha)}\right)\tan 2\phi$$

where $dx$ is the displacement in x on PSD B, $dy$ the displacement in y on PSD B, $\Delta x$ the displacement in x on PSD A (also the linear displacement between the plates in x), $\Delta y$ the displacement in y on PSD A, $\alpha$ the initial angle the laser takes towards the mirror opposite PSD B relative to the normal to the surface at PSD B, $\theta$ the tilt about the y axis, and $\phi$ the tilt about the x axis.

However, it was later found that these complete expressions for the X/Y tip and tilts were too complicated and nearly impossible to practically calculate, at least with a computer running standard MATLAB. As such, further simplifications were made (again, see the XACT Geometry Report for details) to make the expressions practical for typical use. As before, it was found that, with values that would be reasonable in the application, the effects of certain portions of the equations were too small for the finite resolution of the PSDs to detect. The final expressions we used are:

$$dx = \frac{\left(\frac{l}{\cos\alpha} + \frac{(r-\Delta x)\sin\theta}{\sin(90-2\theta-\alpha)}\right)\sin(2(\theta+\ \alpha))}{\sin\,(90-2\theta-\alpha)} - \ d$$

$$dy = \left(l + \frac{(r-\Delta x)\sin\theta\cos\alpha}{\sin\ (90-\theta-\alpha)}\right)\tan 2\phi$$

With these simplifications made, it was possible to compile a table of values that linked complete sets of X/Y displacements and X/Y tip and tilts to a set of PSD readings. Unfortunately, due to time constraints, we were unable to generate a complete, working, and effective system to automatically look up these values from our table or compare them to a best fit system of some sort. Optimally, we would derive a best fit equation from the table of values and use that to calculate approximate tip/tilts to an acceptable accuracy in real time.

## Position Sensitive Photodiodes

**Figure 4: PSDs used in testing system**

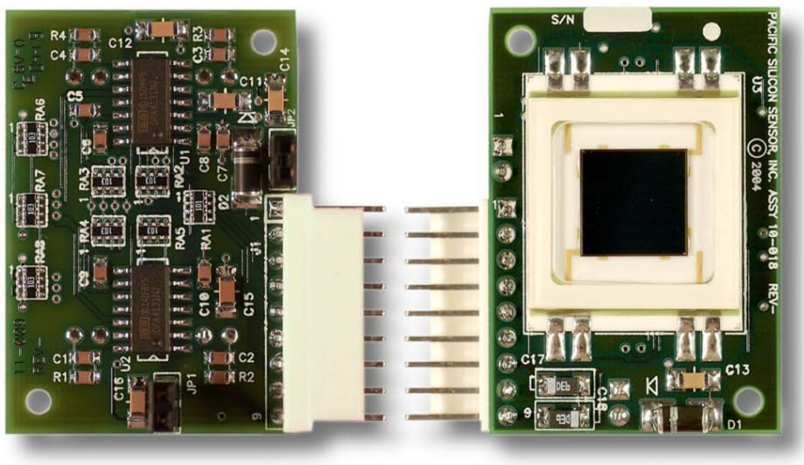

For our testing we used two DL100-7PCBA3 dual-axis PSDs manufactured by Pacific Silicon Sensor Incorporated. These sensors have an active region of one square centimeter and include integrated sum and difference amplifiers.

### Principles of Operation

Position sensitive photodiodes work using the same principles as typical photodiodes. They are essentially a reverse biased P-N junction photodetector. When photons of sufficient energy strike the active PSD area, electron-hole pairs are created and current flows. This current is directly proportional to the intensity of the incoming light. There are four electrodes connected to the sensor (two on the x-axis and two on the y-axis). The current through these electrodes is inversely proportional to the distance from the electrode to the centroid of incoming light. The position of the centroid can be determined by comparing the currents at each electrode. The sensors we are using have integrated sum and difference circuitry, greatly simplifying their application. The devices simply output a voltage corresponding to the position of the centroid of the incident light (centered around 0 V). This also corrects for ambient light, as it will simply appear as a current source in the center of the PSD. For light sources with varying intensity, it is important to take into account the total current through the device. This is done by including the sum outputs from the sensor. More specifics can be found by referring to the PSD datasheet.

### Calibration

As described in the previous section, the PSDs output a voltage corresponding to the position and intensity of incoming light. However, to be able to use these values, we must correlate them to real-world measurements. To do this, we used a Clausing Kondia mill with a 2-axis CNC Accurite Controller (4 micron resolution). This was the most accurate measuring device available to us, and it allowed us to precisely characterize the PSD response over the entire active area. We mounted the test PSD horizontally in a vise, and attached an appropriate power supply. We statically mounted the laser about 1 foot away from the sensor such that the incident light was perpendicular to the sensor. To measure the outputs we used a mixed signal oscilloscope from Tektronix. We manually recorded the displacement and PSD outputs across the device.

**Figure 5: PSD Calibration Setup on Mill**

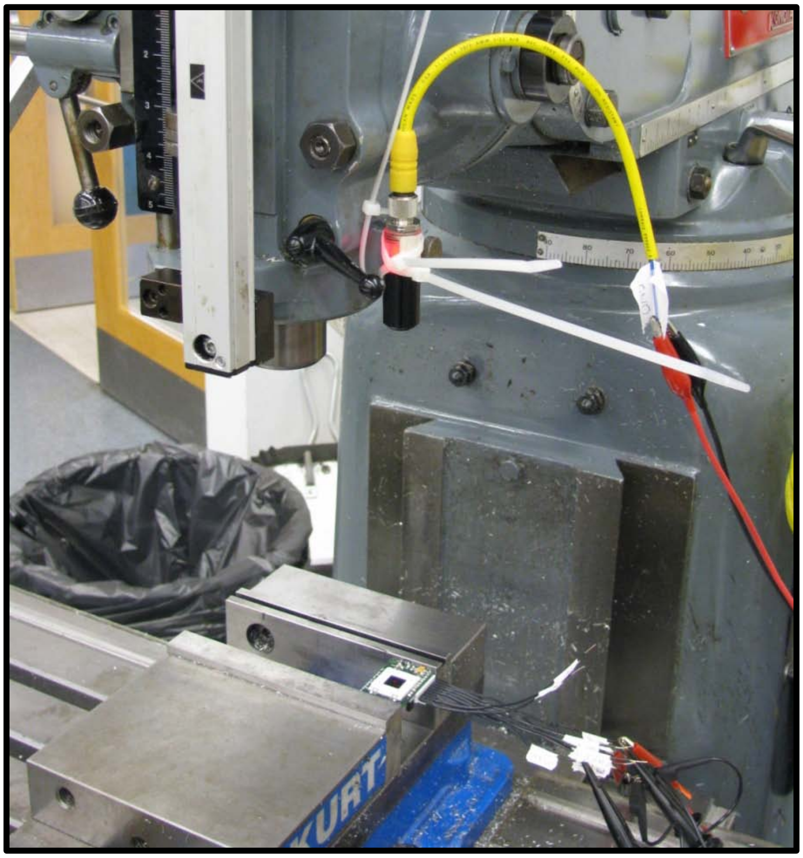


The results, shown in Figure 6, show a perfectly linear response from the PSD in both dimensions (as expected).[1] We observed a very fast response time, little noise, and noted that all of our results were repeatable. Using the data we collected we calculated a best fit line for each axis. In particular, we were interested in the PSD output to displacement conversion. We found that this was around 1.805 microns/mV for the x-axis and 1.774 microns/mv for the y-axis.[2]

[1] Please note that the axes are purposely flipped. This is because, while we calibrated the system with the PSD output as the independent variable, in our final setup we wanted the displacement to be the independent variable.

[2] x-axis best fit: 1.804969777523007x + 23.30701938082171

y-axis best fit: 1.774075453261690x + 7.695920005596407

**Figure 6: Mill Calibration Results for X-Axis and Y-Axis**

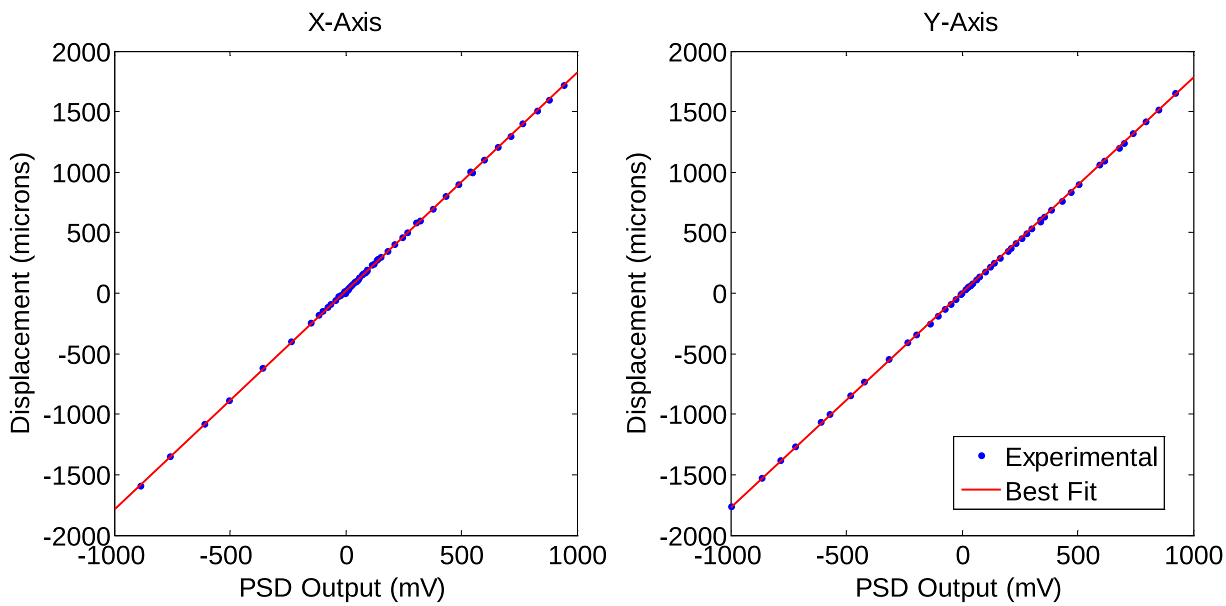


In the case that the intensity of the beam changes during flight, one must take into account the total, or sum, current through the device. The PSD datasheet indicates that the output voltage should be normalized by dividing by the SUM voltage for the layer (x or y) being measured. The results of applying this to our calibration data are shown in Figure 7. However, due to the unlikelihood of beam intensity changes during flight and the significant difference between applying this to the x and y axes, we do not recommend taking into account the total current. It simply becomes another source of error and increases the necessary acquisition time.

**Figure 7: Normalized PSD Outputs[3]**

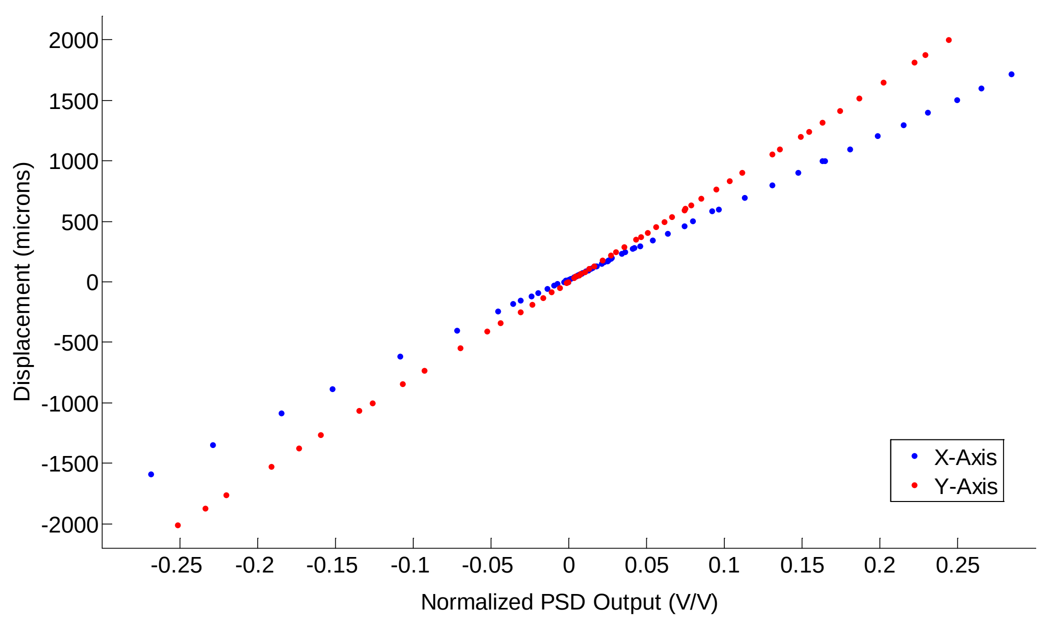

## Testing Apparatus

With Olin College not having an existing optics lab, testing of the system could not be done to the accuracies that were specified by conventional means. To easily and reliably displace the sensors by fractions of millimeters and arcminutes would not have been feasible, so a different system was developed. Instead of moving the rig by a specific amount, the calibrated PSD voltage and displacement curves found on the mill would be used to determine displacements. The rig would then only have to hold the PSD steady while measurements were taken, rather than having to be steady and minutely adjustable. Since we were determining resolution, a steady rig was all that we needed, as long as the recorded output could be verified with the mill calibration data. With this in mind, a testing rig was developed that allowed for all four needed freedoms of movement, with every other restricted.

The overall setup of the adjustable portion of the testing rig, was specifically designed for stability and ease of construction, rather than extreme accuracy. The most important goal was to create a rig that had the required four dimensions of freedom, but no more. To do this, the rig was broken down into two sections, the linear displacement portion, and the angular displacement portion. For linear displacement, a heavy aluminum block sat in a milled track, with the ability to slide up and down, left and right. However, the track restricted the ability to move forward or back. This block's weight, could then be used with set screws to lock the linear displacement. Angular displacement was even simpler, with a pivoting tube for one dimension, and a rotating tube inside the first for the other. These two major pieces allowed for all the needed displacements and no more, while only relying on weight and set screws. This design can be seen in Figure 8.

**Figure 8: CAD Design of Testing Apparatus**

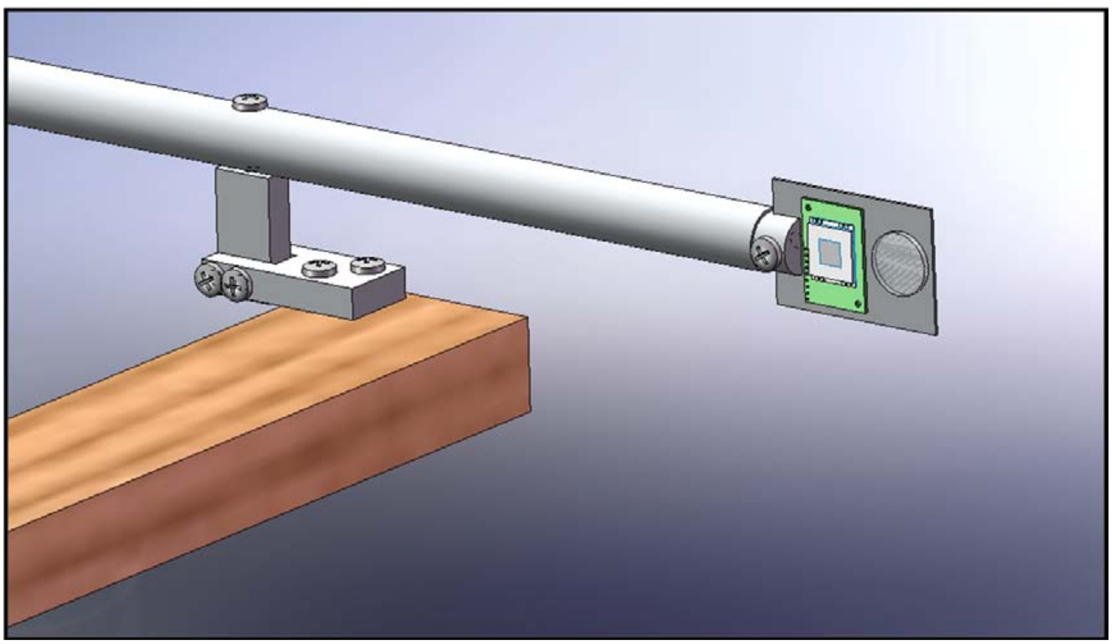

On the other end of the rig, the optical breadboard was assembled using primarily high grade optical components provided to us by our mentor at Goddard. Using the mirror and beam splitter mounts we were able to set up the required geometry very quickly. However, while the mirrors and beam splitters had specific mounts, the PSD and laser did not. To hold these two components in place, adapters were designed and laser cut from Delrin plastic, to hold them in place. With these small adapters, the breadboard end of the rig was easily assembled to specification and minutely adjusted using the inherent precision of the optical mounts. The adapters can be seen in Figure 9 and Figure 10 while the breadboard is shown in Figure 11.

**Figure 9: Breadboard Mount for PSD**

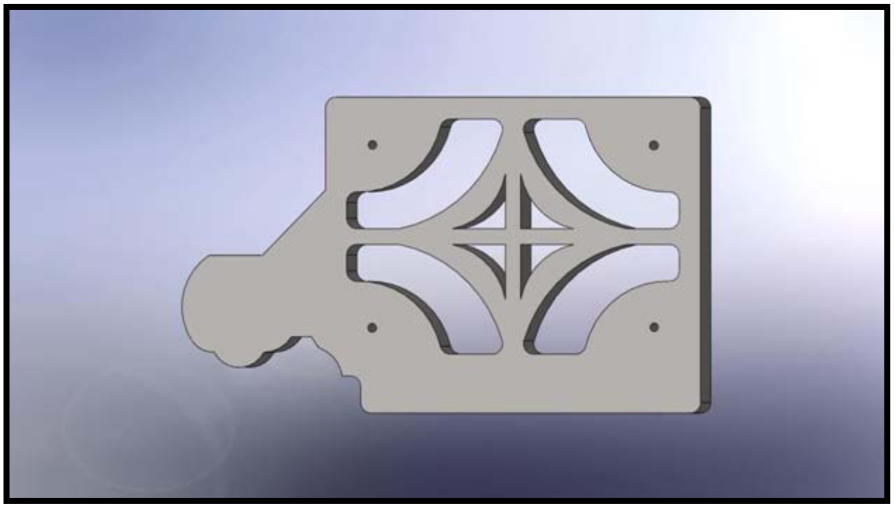

**Figure 10: Breadboard Mount for Laser**

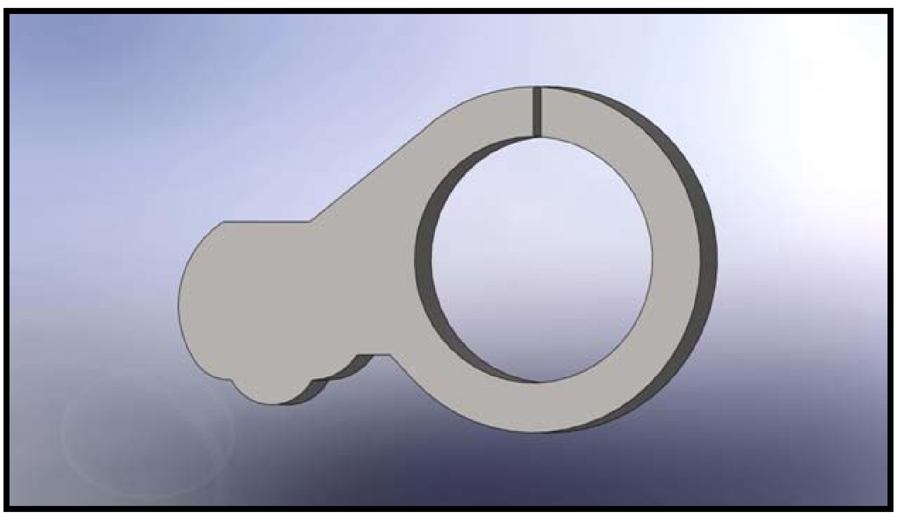

Figure 11: Breadboard Setup for Testing PSD

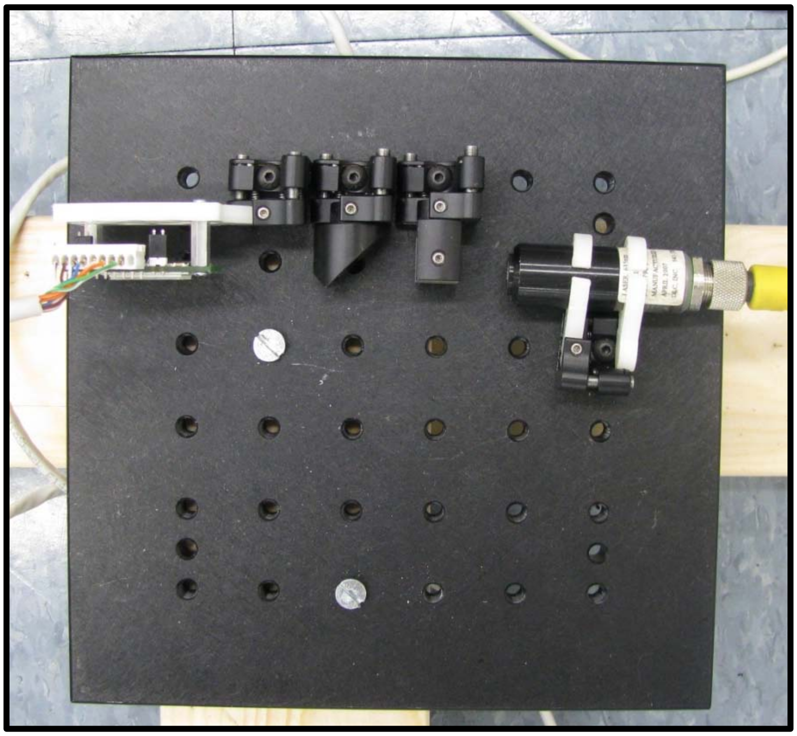

Figure 12: Full Physical Testing Setup

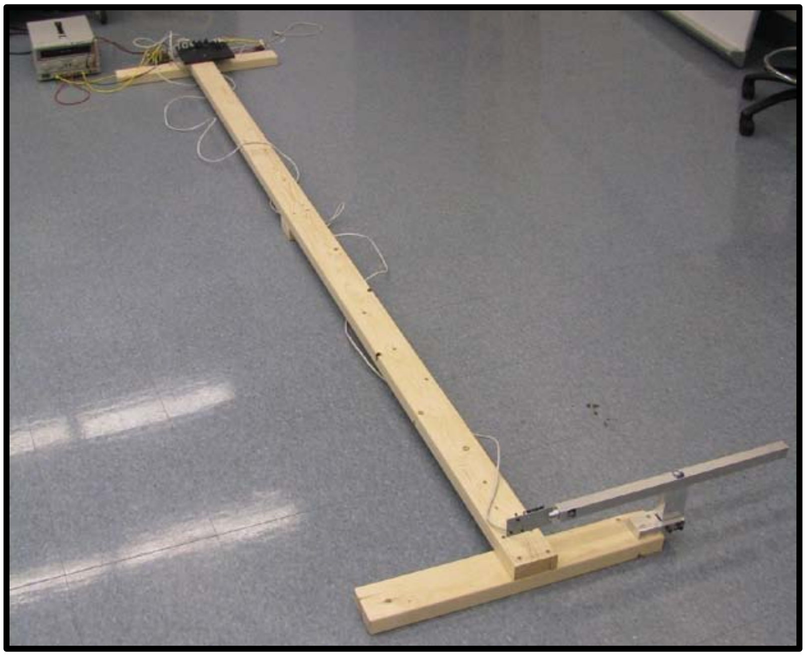

The final rig contains the breadboard and PSD holders previously described. Since minute adjustments were infeasible and the goal was stability, the two major sections were simply screwed into a solid wooden base to keep alignments constant for the proof of concept testing.

## Circuitry

In order to test our system we developed a data-logging device to take the voltage values supplied by the PSDs and transfer them to the computer for processing. Figure 13 shows the basic setup of the device.

Figure 13: Schematic of Data Flow

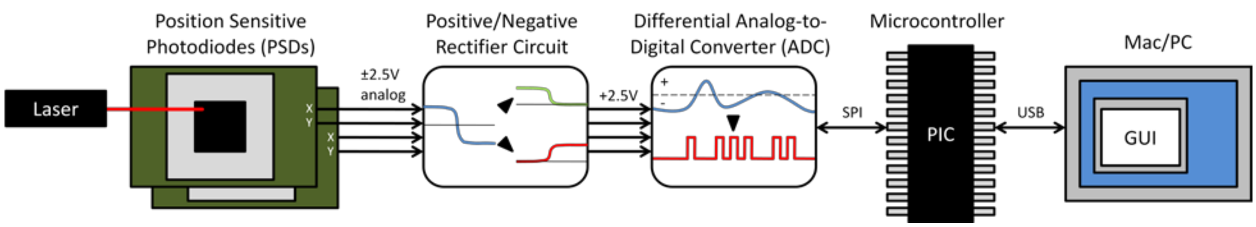


The PSDs output a voltage from -2.5 V to +2.5 V corresponding to the centroid position of incoming light (as described in the section on Position Sensitive Photodiodes). This voltage is then passed through a positive and negative rectifier circuit. These make all of the voltage signals positive so that they can be read by a 12-bit differential analog-to-digital converter (ADC). Depending on whether the positive or negative rectified line is higher, it determines the sign of the reading. The ADC converts the analog signal into a digital value with a precision of 0.61035 mV. This value is then passed on to a PIC microcontroller, which communicates to Mac or PC using the low-speed USB protocol.

Early testing using an oscilloscope showed that output values from the PSDs ranged from around -2 V to +2 V. This allowed us to gage the accuracy needed for the ADCs. The most important aspect here is to use a differential ADC, so that we can determine the sign of the readings. Note that you can increase the precision of the ADCs by adjusting the reference voltages or amplifying the input signal. This amplifies the small changes in sensor readings, making them easier to read out. It will also, however, amplify the noise in the system. We included room for an optional first-order low-pass filter, but hardwired past it as we can apply much better digital filters to our data after the fact.

## Interface Board

**Figure 14: Printed Circuit Board for Interfacing PSDs and Computer**

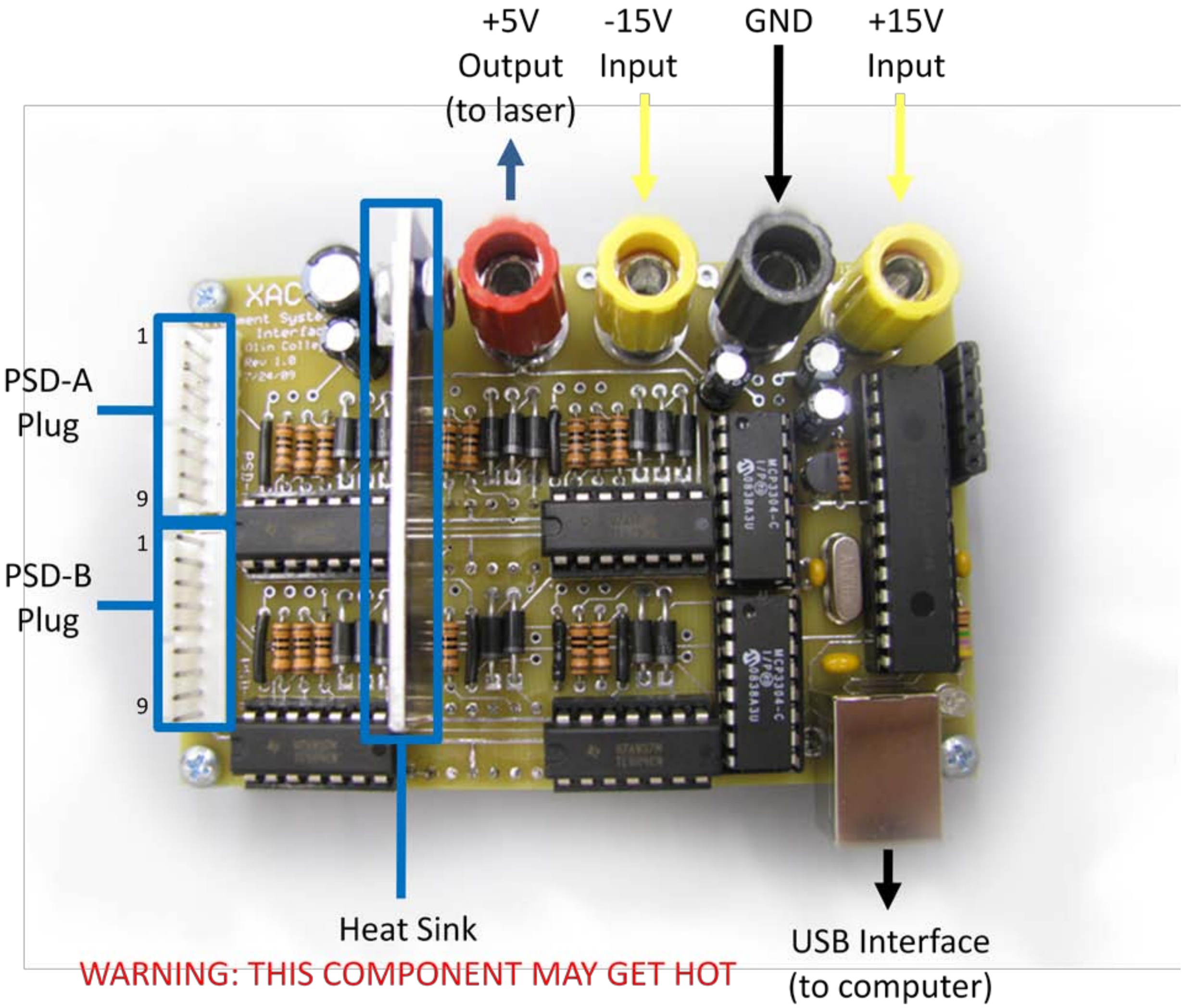


Figure 14 shows the interface board that we created for our tests. It requires a ±15V input from a regulated source in addition to ground. It should not draw more than 500 mA. Do not apply more than, ±18V as it may harm the PSDs. The board has two plugs for the cables that connect to the PSD. We used Category 5 cable and 2.54mm (.100") pitch KK® Crimp Molex connectors to connect the PSDs to the board. Note which PSD is connected to each input and the pin ordering. The board uses a 5 V linear regulator to power the PIC microcontroller and ADCs (and optionally the laser). Due to the large voltage drop required and non-negligible current drawn, the regulator may get hot.

## Code

The data acquisition and processing are controlled by the GUI for xact.py. Once the “Start” button is pressed, the computer begins to control the PIC. At the computer’s command, the PIC reads digital data from the ADC. Each channel is read one after the other, and each reading contains two bytes. One byte contains three 0s, a “sign bit” (1 signifies negative, 0 signifies positive), and the four most significant bits of the reading. The second byte contains the eight least significant bits. All readings are stored in a buffer on the PIC until every ADC input has been read. The buffer is then sent to the computer via a USB cable.

Once the binary data reach the computer, they are processed two bytes at a time (one reading at a time). The computer takes each two-byte pair and converts it back into a signed Base-10 number between 0 and 4096. The component readings are divided by the sum readings (see datasheet: http://www.pacific-sensor.com/pdf/DL400-7PCBA.pdf), and appropriate scaling is performed to produce the final values in microns. These values, along with a timestamp, are written by the computer to a file named “data.txt”. The format is as follows:

**Table II: Organization of data.txt**

| | | | | |
|---|---|---|---|---|
| Time (seconds since 1970) | PSD-A X value (microns) | PSD-A Y value (microns) | PSD-B X value (microns) | PSD-B Y value (microns) |

Once a line is written, the process begins anew for another data capture, which will be written to the next line of the file. The software will overwrite any previous instances of “data.txt”, so old data files should be renamed. Pressing the “Stop” button pauses data acquisition; pressing “Start” again will cause the computer to resume writing to the current data.txt file. The file can be opened even while the program is running, and it will be saved in its final form when the program is closed.

## Results

We are using a 12-bit ADC (plus sign bit). This gives us 4096 divisions between 0 V and 2.5 V (using an external voltage reference). This corresponds to a nominal precision of 0.61035 mV (or around 1.1 microns). For the system to function, we need to be able to resolve .1 mm. For our testing purposes, we wanted to make sure that the value is constant (does not drift) and is not to noisy. To do this, we aligned the laser on our testing apparatus and ensured that the system was rigid. Using our interface board, we collected the data from the two PSDs over an extended period. In our longest test, we found that the system actually had two states through the run: a low-noise period and a high-noise period. The results for each are shown in the following figures. It is important to note that even the data from the high-noise period is well within limits we need.

**Figure 15: PSD Consistency in Low-Noise Period**

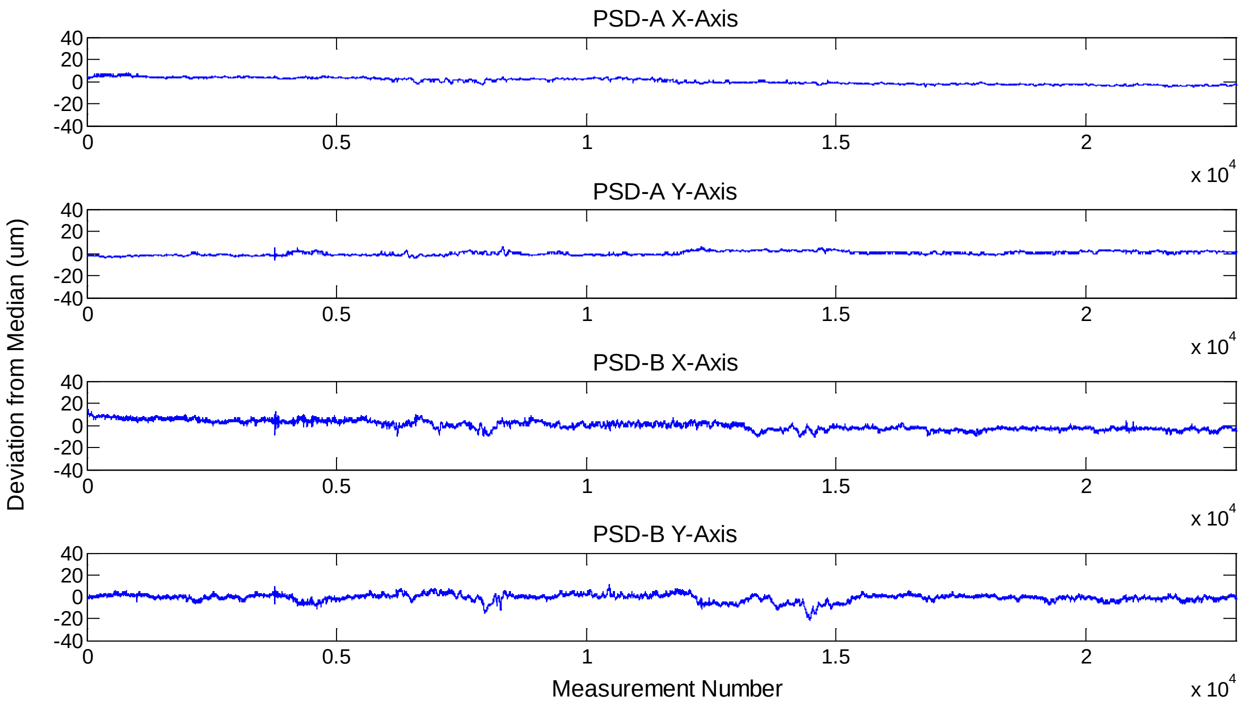


**Table III: Low-Noise Error Analysis**

| Sensor | Dimension | Standard Deviation | Maximum Deviation |
|---|---|---|---|
| PSD-A | X-Axis | 2.91 microns | 7.71 microns |
| PSD-A | Y-Axis | 1.65 microns | 6.50 microns |
| PSD-B | X-Axis | 4.09 microns | 15.42 microns |
| PSD-B | Y-Axis | 3.48 microns | 21.66 microns |

Figure 16: PSD Consistency in High-Noise Period

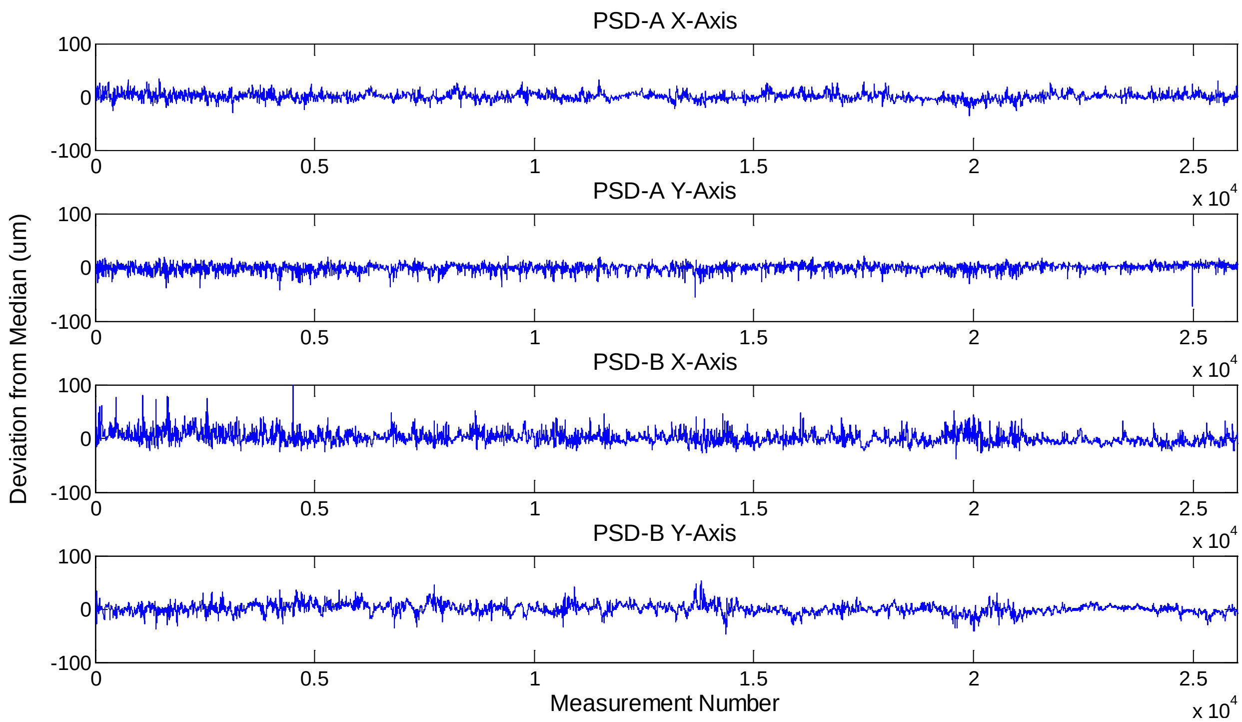


Table IV: High-Noise Error Analysis

| Sensor | Dimension | Standard Deviation | Maximum Deviation |
|---|---|---|---|
| PSD-A | X-Axis | 6.544 microns | 36.35 microns |
| PSD-A | Y-Axis | 6.222 microns | 71.47 microns |
| PSD-B | X-Axis | 10.391 microns | 99.15 microns |
| PSD-B | Y-Axis | 8.830 microns | 53.06 microns |

Note: These results have not been filtered in any way. The application of a digital low-pass filter can eliminate outliers and clean up the results.

## Laser Dispersion

In our testing, we found that the laser, while nominally a single "point" of parallel photons, was dispersed into additional waves and spots through interactions with the optical equipment and its own casing. This should not greatly affect the readings from the PSD; as long as the additional light remains constant it will simply shift the observed centroid of the incoming light to reflect the contributions from the dispersed and/or reflected light. Images of this effect can be seen in Figure 17.

**Figure 17: Examples of laser spot-size on PSD**

This problem can be avoided by using a higher quality laser with a smaller spot size in the final design. Another option is to concentrate the laser beam using some sort of lens. This both reduces the dispersion of the laser beam and increases the intensity at the centroid. We ran a quick test using a simple lens in the lab. We found that this resulted in *significantly* less variation in the readings. We recommend further tests to see if this is feasible in the final system.

## Spaceflight Considerations

We believe that our system should easily and accurately give the necessary data, however, there are special considerations that must be taken into account for any equipment going into space. For a sounding rocket, these issues revolve mostly around the intense launch conditions.

The primary considerations during launch are increased g-forces and vibration from the rapid ascent of the sounding rocket. These forces have the potential to damage the sensor, specifically the attachments of the thin transparent plate over the sensor, which could cause distortions or allow moisture or other interfering or damaging elements to reach the sensor. Investigation into the physical characteristics and tolerances of the PSD is recommended prior to launch.

The main consideration during flight is the operational temperature range of the PSD. It is certified for an operating temperature between 0 and 70 °C, with a preferred temperature of at or below 25 °C. This temperature is not necessarily a given in sounding rocket flight, and thus temperature regulation may be necessary for the sensor to properly function in flight, assuming the same PSDs we tested are utilized.

## System Improvements

Though the system provided meets all specifications and serves as a successful proof of concept, there are various areas that could be improved in the final implementation. Laser light, though focused, does diffuse a bit over space, and the size of the laser dots on the PSDs decreases the effectiveness of the system. To increase measurement reliability, the laser should be very concentrated so as to make its "dot" as close to an infinitesimally small point as possible. This can greatly reduce noise in the system. Also, system speed could be improved by several different methods. For one, faster components (most notably, a faster microcontroller and ADC) could be used. Additionally, the type of ADC could be changed. An ADC that outputs its values in parallel would provide data more quickly than the current ADC (which communicates with the PIC via a serial interface). This would allow all digits corresponding to a digital reading to be output at once, instead of in series. The use of multiple ADCs would also allow the reading out of several channels simultaneously. Furthermore, if necessary, results can be filtered to eliminate variations that are faster than the expected rocket vibrations. This would be accomplished via a low-pass filter applied to the PSD outputs with an appropriate cutoff frequency. A simple RC filter is included in the schematic; however, it was not implemented in our actual circuit. Finally, an external, regulated 5 V power source could be significantly more efficient than the current linear regulator.

# Appendix – Additional Diagrams, Figures, and Information

## XACT Interface Board Circuit Schematic

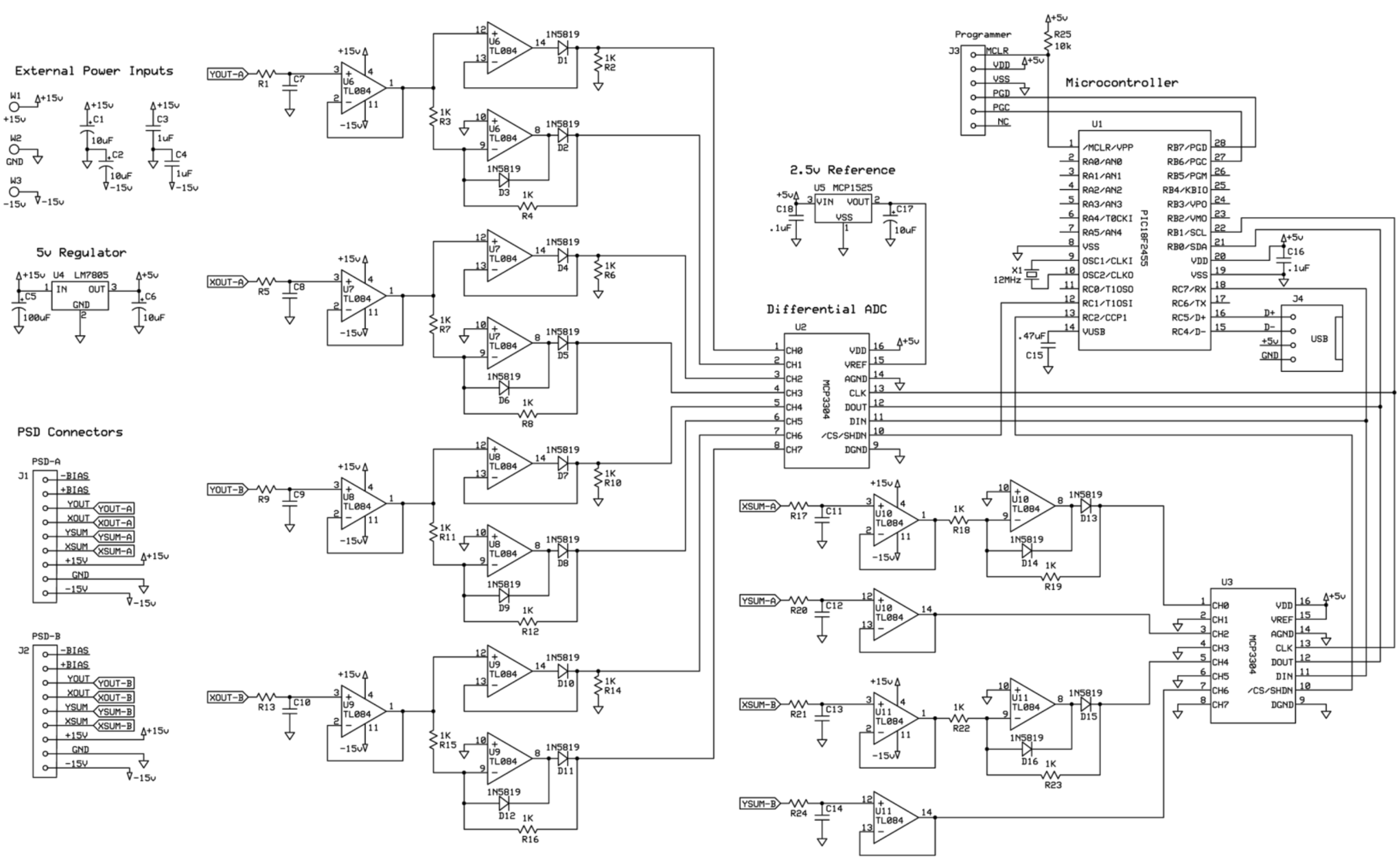

# XACT Interface Board PCB Layout

The circuit board layout was created using the ExpressPCB software package, in coordination with the schematic.

Figure 18: Top Copper Layer

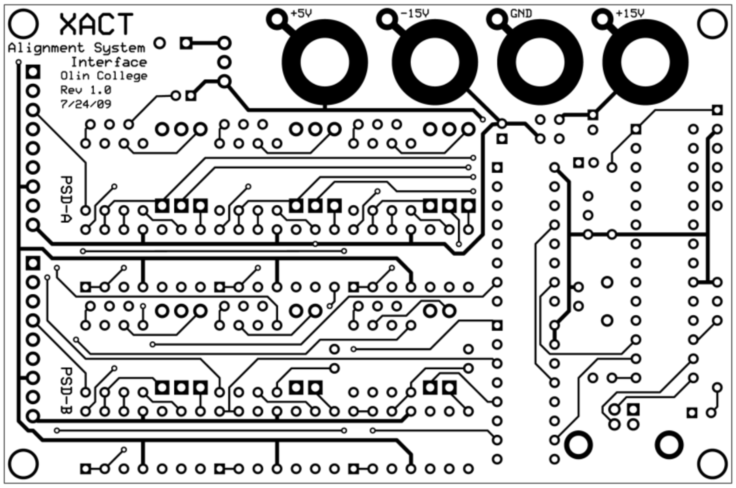


Figure 19: Bottom Copper Layer

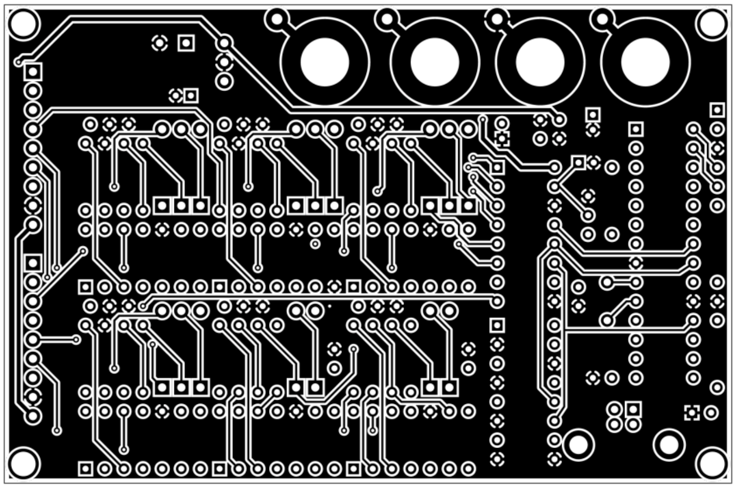

Table 5: Bill of Materials

| Part | Label | Distributer |
|---|---|---|
| 10 uF Electrolytic Capacitor | C1, C2, C6, C17 | Mouser 647-UVR1V100MDD1TD |
| 1 uf Ceramic Capacitor | C3, C4 | Mouser 80-C320C104M5UCA7301 |
| 100 uF Electrolytic Capacitor | C5 | Mouser 647-UVR1H101MPD1TD |
| .47 uF Ceramic Capacitor | C15 | Mouser 80-C320C474M5U |
| .1 uF Ceramic Capacitor | C16, C18 | Mouser 80-C320C104M5UCA7301 |
| 1N5819 | D1-D16 | Mouser 844-1N5819 |
| 1 K Resistor | R1-R24 | Mouser 71-CCF551K00FKE36 |
| 10 K Resistor | R25 | Mouser 71-CCF07-J-470-E3 |

| | | |
|---|---|---|
| USB-B Connector | J4 | Mouser 737-USB-B-S-RA |
| PIC18F2455 | U1 | Microchip Direct |
| MCP3304 | U2, U3 | Microchip Direct |
| LM7805 | U4 | Mouser 512-LM7805CT |
| MCP1525 | U5 | Microchip Direct |
| TL084 | U6-U11 | Mouser 595-TL084CN |
| 12 MHz Crystal Oscillator | X1 | Mouser 815-ABL-12-B2 |
| Binding Posts | W1-W4 | Mouser 565-3760 |

## Test Apparatus Example Setup

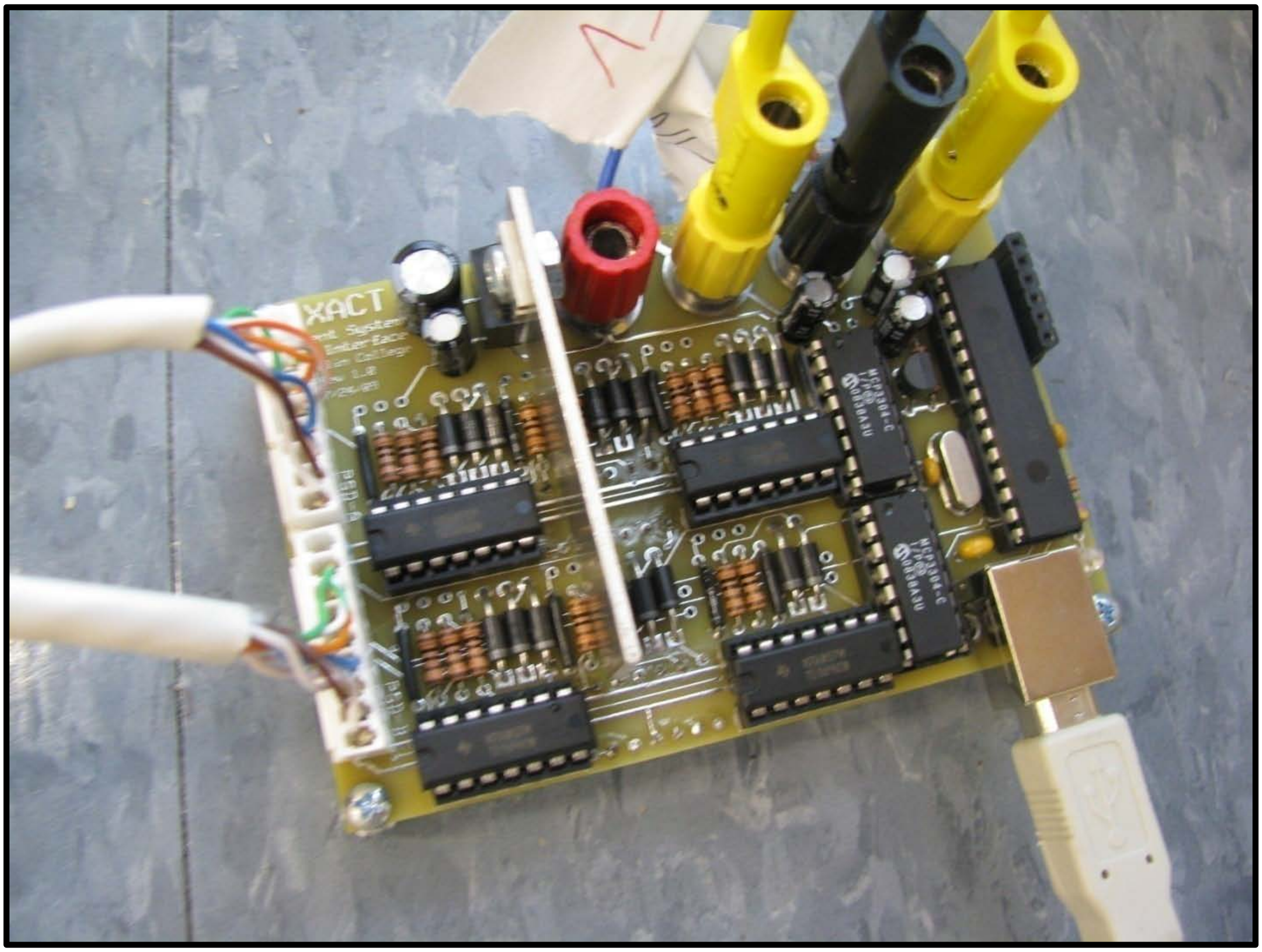


## Acknowledgements

Thanks to Dr. Stephen Holt, Dr. Bradley Minch, and Dr. Keith Gendreau for their generous help and support on this project.

## Concluding Note

As our report documents, we feel that we have provided a successful and effective proof of concept for a laser-based optical alignment system for the XACT sounding rocket program. We have demonstrated the capability of the position-sensitive photodiodes to detect changes of the required magnitude, as well as of our interface's ability to recognize those changes. Furthermore, we elaborated on the possibility of real time solving to find the desired end values of X and Y displacement and tip/tilt from the original PSD voltage readings. In short, we are glad to say that an optical alignment system is feasible for XACT and other sounding rocket programs and that we have provided a basis from which flight-ready systems can be developed and improved.

To close, we would like to thank Dr. Keith Gendreau for the opportunity to work on the XACT Alignment System and for all his help and support for the NASA-Olin Program. Thank you to Dr. Steve Holt as well for all of his fantastic assistance throughout the project and for giving us the chance to participate in the program in the first place. It was a fantastic experience, and we are all lucky to have been a part of it. Thank you.

Clay Gimenez, Project Manager
On behalf of the XACT Team: Raphael Cherney, Daniel Elg, Clayton Gimenez, and Steven Higgins
NASA-Olin 2009